Analysis of Changes in ECG Morphology Prior to In-Hospital Cardiac Arrest Using Weighted Tensor Decompositions

Griet Goovaerts, Martijn Boussé, Duc Do, Lieven De Lathauwer, Sabine Van Huffel, Xiao Hu

***Abstract*— *Objective:* In-hospital cardiac arrests are an important group of cardiac arrests characterized by low survival rates. In order to identify patients at risk, their physiological signals such as the electrocardiogram (ECG) can be monitored in order to detect alterations that can predict arrests. This work presents an analysis of the changes in ECG morphology prior to in-hospital cardiac arrest in different patient groups. *Methods:* We have developed a novel strategy that uses weighted tensor decompositions to extract features from the ECG signal. The use of weighted decompositions allows to take the noise level of the signal into account, leading to a more accurate analysis in real-life applications. After preprocessing and R peak detection, a third-order tensor is constructed for each ECG signal by segmenting the multilead signal in individual heartbeats and stacking them in a three-dimensional manner. The result of the weighted tensor approximation are three factor vectors corresponding to each mode of the tensor which can be used to calculate features that characterize the heartbeat morphology. Changes in these parameters are analysed in two different ways: by detecting significant changes from baseline and by analyzing the dominant trend in the signal. The goal of these analyses is to determine which features change significantly prior to the cardiac arrest and can thus be used to identify and monitor patients in a hospital setting. *Results:* A dataset of 160 patients who experienced a cardiac arrest in the intensive care unit is processed. Patients are divided in three groups depending on the cause of the cardiac arrest. Both analyses demonstrate statistical differences between the three groups. Among others, results show that changes in PR interval length and QRS interval length are discriminative between the different causes of cardiac arrests, together with trends in all interval durations. *Conclusion:* The proposed method is an innovative way of analysing ECG morphology and can be used to characterize ECG signals prior to in-hospital cardiac arrest.**

***Index Terms*— higher-order tensor, canonical polyadic decomposition, weighted least squares, dominant trend, electrocardiogram**

Submitted for review on 30/08/2018. This work is supported by Research Council KU Leuven: C1 project C16/15/059-nD, FWO -: G.0830.14N, G.0881.1. This work was supported by imec funds 2017. European Research Council: The research leading to these results has received funding from the European Research Council under the European Unions Seventh Framework Programme (FP7/2007-2013) / ERC Advanced Grant: BIOTENSORS (no 339804). This paper reflects only the authors views and the Union is not liable for any use that may be made of the contained information. Fonds de la Recherche Scientifique FNRS and Fonds Wetenschappelijk Onderzoek Vlaanderen under EOS Project no 30468160 (SeLMA), Research Council KU Leuven: C1 project C16/15/059-nD, FWO projects: G.0830.14N, G.0881.14N, This work in partially funded by R01NHLBI128679, R18H5022860, R01GM111378, UCSF Middle-Career scientist award, and UCSF Institute of Computational Health Sciences G. G. is a PhD fellow of IWT Vlaanderen (VLAIO). G. Goovaerts, M. Boussé, L. De Lathauwer and S. Van Huffel are with the Department of Electrical Engineering (ESAT), STADIUS Center for Dynamical Systems and Signal Processing, KU Leuven, Belgium (Email: griet.goovaerts, martijn.bousse, lieven.delathauwer, sabine.vanhuffel@esat.kuleuven.be). G. Goovaerts and S. Van Huffel are also with imec, Leuven, Belgium. L. De Lathauwer is also with the Group of Science, Engineering and Technology, KU Leuven Kulak, Kortrijk, Belgium. X. Hu is with the Department of Physiological Nursing and Neurosurgery, Institute for Computational Health Sciences, Affiliate, UCB/UCSF Gradu. D. Do is with UCLA Cardiac Arrhythmia Center, David Geffen School of Medicine, University of California, Los Angeles(UCLA), Los Angeles, CA 90095, USA

I. Introduction

CARDIAC arrest is one of the leading causes of death worldwide. Early identification of patients at risk would therefore be of great benefit to improve patient outcome. One strategy is to continuously monitor vital signs in patients and identify patterns or changes in these signals that are predictive for a later cardiac arrest in that patient. In-hospital cardiac arrests account for approximately 40% of all arrests [1]. Since this type of cardiac arrests has a low survival rate (only 20% of patients survives to discharge [2]) and patients in the hospital can be more easily monitored than in a home environment, they are a preferential group to develop methods for early patient identification. These methods can then be applied to out-of-hospital cardiac arrest populations in the future.

When a patient experiences a cardiorespiratory arrest in a hospital, a *code blue* is called, indicating a medical emergency or a person in need of immediate medical attention. When a patient has an increased chance of deterioration and eventually of cardiac arrest, rapid response teams are called in order to start early interventions to avoid the occurrence of an actual code blue. We will therefore examine how the ECG signal morphology changes prior to a code blue in patients with different causes of cardiac arrest. The identification of ECG features that change significantly before a cardiac arrest would allow a more precise monitoring and could therefore potentially decrease the number of actual code blues. The ECG signal is chosen over other vital signs since it can be measured non-invasively and monitoring equipment is available in most clinical settings.

There have been many studies investigating the immediate mechanisms visible on ECG signals that lead to a cardiorespiratory arrest [3]–[5], but changes over a longer timescale (multiple hours before the cardiac arrest) are less well-studied.

Previous studies focused on bradyasystolic cardiac arrests [6], [7] or heavily relied on manual measurements [8]. This study extends the analysis to other causes of cardiac arrest, using automated methods that need a minimum of user interaction. This makes them more useful for future use in clinical practice. We have developed a method that uses tensor decompositions to extract information from the ECG signal. Tensors are multiway generalizations of vectors and matrices that have been widely used in different domains [9]–[11]. In ECG signal processing they have been successfully used for T Wave Alternans detection [12], [13], characterization of myocardial infarction [14] and irregular heartbeat detection [15], [16]. They have many advantages compared to traditional matrix-based methods, especially when dealing with signals that are fundamentally multidimensional such as multilead ECG signals. Tensor methods allow a simultaneous analysis of all leads at once, taking into account all information stored in the signal. Furthermore they yield unique results under mild conditions [9]–[11]. In this paper we use weighted tensor decompositions, which allow us to incorporate prior knowledge about the signal quality in the tensor decomposition in the form of a weight tensor [17]. When choosing the weights properly, they can automatically deal with the noise that is inherent to biomedical signals, leading to a more accurate analysis and making them better suited to work with real-life signals. The method used in this study furthermore uses a computationally efficient weighting scheme [18], which is essential for real-time processing. As such, this work has the following main contributions:

- The application of computationally efficient weighted tensor decompositions to extract ECG features, which permits to correct for lower signal qualities in quasi real-time.
- Development of a noise model to estimate the SNR value of each individual heartbeat.
- The use of different analyses of changes in parameter values prior to in-hospital cardiac arrest
- The inclusion of three different patient groups with different preceding rhythms.

The rest of this paper is structured as follows: The next Section briefly introduces the most important tensor-related concepts necessary in the remainder of this paper. In Section III a short description of the dataset is given. The different steps of the developed method are described in Section IV. Sections V and VI contain respectively the results and discussion, after which the paper is concluded in Section VII.

II. Tensor prerequisites

A. Notation and basic definitions

Tensors are higher-order generalizations of vectors and matrices. The order of a tensor is equal to the number of modes, e.g. a vector and matrix have order one and two, respectively. Here, we will work with third-order tensors. In the remainder of this paper, scalars, vectors, matrices and tensors are denoted by respectively lowercase letters (x), bold lowercase letters ($\mathbf{x}$), bold uppercase letters ($\mathbf{X}$) and calligraphic letters ($\mathcal{X}$). Tensors can be indexed by fixing some of the tensor's indices. This way mode-n fibers are defined by fixing all but the nth index and mode-(m,n) slices by fixing all indices except m and n. This ways, the columns and rows are respectively the mode-1 and mode-2 vectors.
The outer product and Hadamard or entry-wise product are denoted by $\otimes$ and $*$ respectively. $||.||_F^2$ represents the Frobenius norm of the tensor, defined as the square root of the sum of the squared magnitude of its elements. A rank-1 tensor is defined as the outer product of non-zero vectors.

B. Canonical Polyadic Decomposition

Tensor decomposition methods decompose a tensor in a sum of low-rank terms. A well-known method with interpretable results is the Canonical Polyadic Decomposition (CPD) [19] which decomposes a tensor in a minimal sum of rank-one terms. For a third-order tensor $\mathcal{T} \in \mathbb{R}^{I\times J\times K}$ it can be expressed as:

$$\mathcal{T} = \sum_{r=1}^{R} \mathbf{a}_r \otimes \mathbf{b}_r \otimes \mathbf{c}_r$$

with R the total number of components in the decomposition and $\mathbf{a}_r \in \mathbb{R}^I$, $\mathbf{b}_r \in \mathbb{R}^J$ and $\mathbf{c}_r \in \mathbb{R}^K$ for $r = 1, \ldots, R$ the factor vectors. The determination of R is a non-trivial problem, especially for tensors which contain noise. Mathematically, a CPD can be computed by solving the following optimization problem:

$$\min_{\mathbf{A},\mathbf{B},\mathbf{C}} \frac{1}{2}||\mathcal{T} - [\![\mathbf{A},\mathbf{B},\mathbf{C}]\!]||_F^2$$

with $\mathbf{A}$, $\mathbf{B}$ and $\mathbf{C}$ the factor matrices that consist of the factor vectors $\mathbf{a}_r$, $\mathbf{b}_r$ and $\mathbf{c}_r$. The CPD can be computed in many ways [9], [17], [20]. Here we use an optimization-based method that uses nonlinear least-squares (NLS) [21].
One of the main advantages of tensor decompositions compared to matrix-based methods is that the resulting components are unique under mild conditions (up to permutation and scaling). A general framework for uniqueness properties of third-order tensors is presented in [22]. This means that no additional constraints have to be imposed on the data or factor matrices which is required for matrix decompositions such as Principal Component Analysis (orthogonality) or Independent Component Analysis (independence).

III. Data

The dataset contains multilead ECG signals of patients that experienced a code blue due to a cardiopulmonary arrest in the intensive care units of the Medical Centers of the University of California in San Francisco (UCSF) and Los Angeles (UCLA). All code blues occurred between 2013 and 2015. For all patients, information is provided about the date and time of the code blue, the type of cardiac arrest and whether they survived the code blue/and or survived to discharge. Patients were divided in three different groups depending on the preceding rhythm (prior to the arrest):

1) Ventricular tachycardia or ventricular fibrillation (VT/VF)
2) Asystole
3) Pulseless Electrical Activity (PEA)

TABLE I: Number of patients with preceding rhythms in the dataset.

Cardiac arrest	# patients	%
VT/VF	33	20.6%
Asystole	28	17.5%
PEA	99	61.9%

For each patient, ECG signals from the last 24 hours before the code blue occurred were extracted. However, not all patients were continuously monitored over these 24 hours. Only patients with a total ECG length of more than 3 hours were included in the study. Additionally, patients of which the cause of cardiac arrest was not known or dubious were also excluded for analysis.

The final dataset contains 160 recordings with a sampling frequency of 240 Hz. The signals from UCSF contain 7 channels: I, II, III, V, aVR, aVL and aVF, those from UCLA are measured with 4 leads. The number of patients in each cardiac arrest group is summarized in Table I.

IV. Methods

Our method consists of five different steps: 1) The signals were first preprocessed to remove major noise sources and detect R peaks. 2) The two-dimensional signals were then transformed into a third-order tensor, which was subsequently 3) decomposed to extract a template heartbeat. 4) This heartbeat was used to derive seven parameters 5) which were finally analysed in two different ways.

A. Preprocessing

Some ECG recordings contained corrupted portions, which were visually detected and deleted. All signals were then preprocessed channel-by-channel. First a Butterworth high-pass filter with order 2 and cutoff frequency 0.5 Hz was applied to remove baseline wander. The filter was applied twice, first in forward and afterwards in backward direction to remove phase distortion so the order is effectively doubled to 4. The filter parameters were chosen in order to minimize deformations of the ECG signals, as shown in [23]. Then the signals were normalized by calculating the modified z-score z', which is more robust to outliers than the standard z-score [24]

$$z'_i = \frac{0.6745(x_i - \tilde{x})}{MAD}$$

where $\tilde{x}$ denotes the median and MAD the median absolute deviation of the signal. R peaks were detected using a multilead extension to the Pan-Tompkins algorithm that fuses R-peaks detected in separate channels [25].

B. Tensorization

Multilead ECG signals are typically collected in a matrix with dimensions *channel* x *time*, i.e. each row of the matrix contains the ECG time signal for a particular channel. They therefore have to be tensorized (i.e. transformed into tensors) prior to using tensor decomposition techniques. Many tensorization approaches such as segmentation, hankelization and lownerization exist, and the optimal choice often depends on the application and characteristics of the signal at hand [26]. We tensorized this ECG data matrix into a third-order tensor with dimensions *channel* x *time* x *heartbeats* where each mode-two fiber represents one heartbeat in one channel. First, the signals were segmented in individual heartbeats of length I, obtaining J heartbeats for all M channels. Next, we stacked all heartbeats in the third mode, resulting in a third-order tensor $\mathcal{T} \in \mathbb{R}^{M \times I \times J}$. Segmentation was done here by taking a fixed-size segmentation window symmetrical around the R peak. The window length is $1.6RR$ (with RR the mean RR interval length).
All signals were processed with a sliding window of 100 heartbeats without overlap between subsequent windows. We constructed, decomposed and analysed a tensor for each window, which allowed to capture the dynamic ECG changes over time. The result of the tensor construction was thus one tensor $\mathcal{T}$ for each 100 beat window. Each tensor had three modes: the first mode was the spatial mode which corresponded to the different ECG leads in the signal. The second temporal mode showed the time course of the individual heartbeat and had a varying length equal to the length of the segmentation window for each tensor. Finally, the third mode was the heartbeat dimension with a fixed length of 100.

C. Tensor decomposition

1) Weighted CPD: As explained before, CPD writes a tensor $\mathcal{T}$ as a sum of rank-one terms. Here we used an alternative way to compute the CPD, namely Weighted CPD (WCPD) which uses *weighted* least-squares instead of regular least-squares. WCPD permits the incorporation of prior knowledge about the signal quality in the tensor decomposition, giving lower weight to entries with higher noise levels. This is done by introducing a weight tensor $\mathcal{W} \in \mathbb{R}^{M \times I \times J}$ with the same dimensions as $\mathcal{T} \in \mathbb{R}^{M \times I \times J}$ into the optimization problem II-B. Each entry of $\mathcal{W}$ contains the weight for the corresponding entry of $\mathcal{T}$. A detailed explanation of the weight tensor construction follows in the next paragraph. The new optimization problem is then:

$$\min_{\mathbf{A},\mathbf{B},\mathbf{C}} \frac{1}{2} ||\mathcal{W} * (\mathcal{T} - [\![\mathbf{A}, \mathbf{B}, \mathbf{C}]\!])||_F^2$$

The optimization problem was solved using a novel Weighted Least Squares approach (WLS) where the weight tensor is modelled by a polyadic decomposition (as in Equation II-B), enabling efficient weighting. The computational details of the WLS algorithm can be found in [18].
In previous applications where tensor decompositions were used to decompose and analyse ECG signals, a CPD rank of one was shown to lead to good results [12], [15]. The same approach was used here. This means that the tensor $\mathcal{T}$ was compressed into a single rank-one term, consisting of factor vectors $\mathbf{a}_1 \in \mathbb{R}^M$, $\mathbf{b}_1 \in \mathbb{R}^I$ and $\mathbf{c}_1 \in \mathbb{R}^J$

2) Construction of weight tensor: The weight tensor $\mathcal{W} \in \mathbb{R}^{M \times I \times J}$ contains information about the signal quality, e.g. entries with higher quality receive higher weights. The quality of ECG signals is reduced by artifacts, which are technical or

physiological. Technical artifacts can be caused by equipment malfunctioning or electrode loosening. During a technical artifact no ECG signal is measured; the corresponding entries in $\mathcal{T}$ therefore receive a weight of 0, effectively eliminating them from further analysis. Physiological artifacts are caused by for example muscle contractions and are superimposed onto the ECG signal, reducing the Signal-to-Noise Ratio (SNR). For signals which do not contain technical artifacts an estimate of the SNR (calculated using a novel SNR model described in the next paragraph and Appendix A) was therefore used as weight. We calculated one weight for each complete mode-2 fiber, e.g. each full heartbeat in each channel. It was thus assumed that the signal quality was the same during the time course of one heartbeat but could differ from channel to channel or between different heartbeats. Hence, the resulting weight tensor $\mathcal{W}$ has rank M, by construction, with M equal to the number of channels in the ECG signal.

a) Technical artifacts: Some typical examples of technical artifacts are shown in Figure 1. They are characterized by extreme signal amplitudes (Fig 1b) and/or very structured patterns (Fig 1a) that are substantially different from physiological signals. Figure 1b includes three seconds of normal ECG signal in the beginning and end as an amplitude reference. Since the artifacts were extremely dissimilar from normal ECG signals, they could be detected with the following straightforward heuristic. A heartbeat was determined to have a technical artifact if at least five samples had either:

1) Modified z-score > 5
2) Modified z-score = 0
3) Constant derivative

The weights of technical artifacts were fixed to zero, as described in the previous paragraph.

b) Physiological artifacts: As explained earlier, we used an estimate of the SNR of a heartbeat as weight in the case of physiological artifacts. We developed a SNR model based on the MIT-BIH Noise Stress Test Database [27] which contains ECG signals with standardized SNR values. The model contained 8 different features found in the literature that have been proven successful in calculating the SNR of an ECG signal:

1) Skewness
2) Kurtosis
3) Power in 6 different sub bands: 0-10 Hz, 10-20 Hz, 20-48 Hz, 48-52 Hz, 52-100 Hz, 100-120 Hz

A detailed explanation of the construction and validation of the SNR model can be found in Appendix A.

D. Parameter calculation

The output of the weighted tensor decomposition are 3 factor vectors a_1, b_1 and c_1, corresponding to each dimension (or mode) of the tensor. Examples of each factor vector for a typical ECG signal are depicted in Figure 2. The mode-1 vector a_1 (Fig 2a) shows the distribution over the different ECG channels. The mode-2 vector of the temporal dimension b_1 can be seen as a template heartbeat for all heartbeats in that window (Fig 2b). The mode-3 factor vector c_1 shows the differences among all heartbeats in a window (Fig 2c). Since the analysis focused on the changes in ECG morphology, the mode-2 factor vector was used for further analysis. All factor vectors are by definition unique up to scaling (see also Section II.B). Since there is only one term here, there is no permutation ambiguity. In order to remove differences in scaling between different tensor decompositions, all vectors were first normalized to unit length, b_1 was then rescaled by multiplying it with λ [9]

$$\lambda = ||a_1||.||b_1||.||c_1||$$

with $||a_1||$, $||b_1||$ and $||c_1||$ the original norms of the vectors.

As explained earlier, the mode-2 factor vector corresponds to the model heartbeat in the ECG signal. Standard techniques could thus be used to automatically detect the individual ECG waves. Here, we used the wavelet-based ECG delineator developed by Martinez et al. [28] to extract the locations of the P wave peak, Q wave, R peak, S peak and T peak. Only the peak of the P and T wave were detected since the begin and end points of these waves are often hard to distinguish. All annotations were inspected visually and adjusted where necessary. 7 different metrics were calculated for each analysed window:

1) Mean heart rate in bpm (*HR*), calculated from the length of b_1 (l) which is equal to the segmentation window for each tensor (see Section IV-B):
$$\left.\begin{array}{l} l = 1.6RR \\ HR = \frac{60.fs}{RR} \end{array}\right\} HR = \frac{60.fs}{l/1.6}$$
with RR the mean RR interval length in samples and fs the sampling frequency of the recording.
2) PR interval in ms (*PR*)
3) QRS interval in ms (*QRS*)
4) QT interval in ms (*QTc*), corrected for heart rate using Fridericia's correction formula [29]
$$QTc = \frac{QT}{\sqrt[3]{RR}}$$
5) Amplitude of the P wave (*pAmp*)
6) Amplitude of the R wave (*rAmp*)
7) Amplitude of the T wave (*tAmp*)

All parameters could be computed from the detected waves by either calculating the differences between the corresponding time stamps (metrics 2-4) or by measuring the amplitude of b_1 at that point (metrics 5-7). Missing values, for example in windows which fully consist of technical artifacts, were imputed by linearly interpolating the parameter values between the last known value and the next known value. Note that since all signals were normalized in the preprocessing stage, the final three parameters do not present the ECG signal in μV, but rather the normalized amplitudes. This facilitates comparison among subjects.

E. Analysis of changes in parameter values

Two different analyses were performed. The first one examined the changes of the different parameters compared to a baseline value in the beginning of the recording. The second analysis looked at the dominant trend in the parameter values.

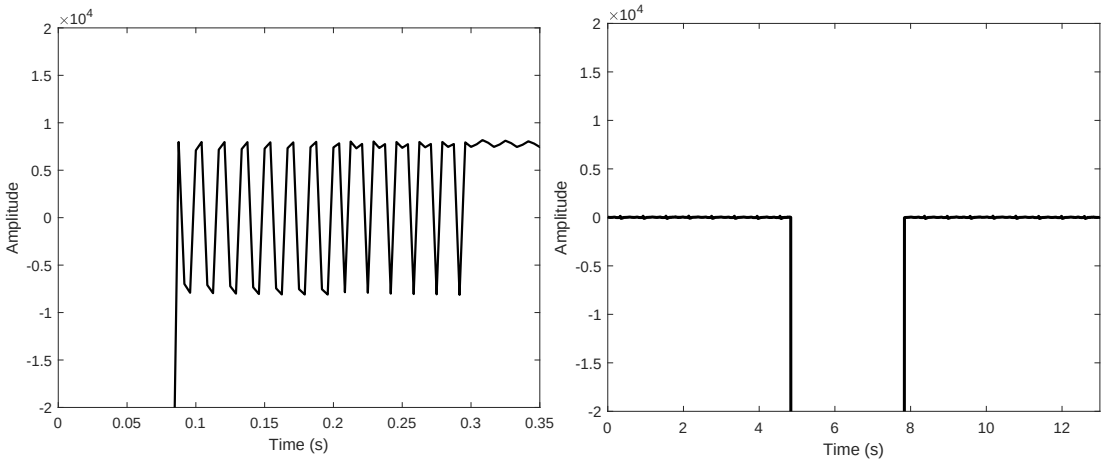

(a) Technical artifact with structured pattern (b) Technical artifact with extreme amplitude

Fig. 1: Two examples of typical technical artifacts found in the dataset. They can be easily detected and removed by setting their corresponding weights in the weight tensor to zero.

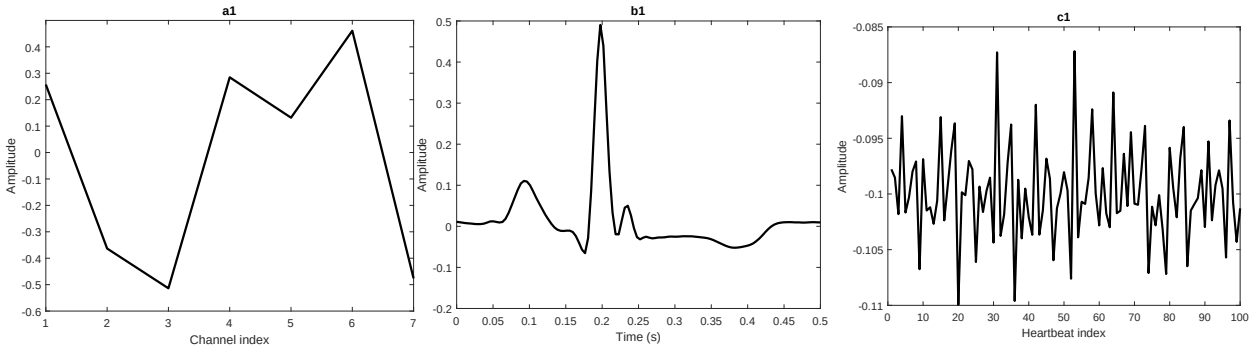

(a) Mode-1 spatial vector a_1 (b) Mode-2 temporal vector b_1 (c) Mode-3 heartbeats vector c_1

Fig. 2: Illustration of the factor vectors of the weighted CPD for a typical ECG signal. Each vector corresponds to one mode of the original tensor $\mathcal{T}$.

1) Changes from baseline: The first analysis detected significant changes from baseline. For each parameter in each patient, an individual baseline value was defined as the median of the first five available values. Each parameter in each analysis window was compared to the baseline value, and changes were considered significant if they exceeded a threshold value for at least 20 consecutive windows or if they were sustained until the time of cardiac arrest, as was defined in [8]. Increases and decreases in parameter values were examined separately. For *PR*, *QRS* and *QTc* a significant change was a >20ms change from baseline value. For *pAmp*, *rAmp* and *tAmp* a change was significant if the amplitude rises or falls larger than 20% from baseline value. For heart rate measurements a difference of 25BPM was detected. All baseline values and threshold values for PR, QRS and QTc interval lengths were chose identical to [8] so results can be compared easily. Threshold values for the other parameters (not analysed in [8]), were defined based on the work by [30] which studies normal variations in the amplitudes of ECG waves during stress testing.

Comparisons between groups (e.g. patients with different causes of cardiac arrest) was performed with a Chi-Square test, which compares proportions between different groups (in this case patients with different causes of cardiac arrest). Since changes of 7 different parameters were tested, correction for multiple comparisons was done with the Benjamini-Hochberg procedure to decrease the false discovery rate [31]. All p-values were ranked in ascending order, and each p-value was compared with its Benjamini-Hochberg critical value c_i to determine significance. c_i was defined as:

$$c_i = \frac{i}{m}Q$$

with i the rank of the p-value, m the total number of parameters and Q the false discovery rate, set to a standard value of 10% in this case as suggested in [32].

2) Dominant trend analysis: Determination of the dominant trend in a signal is a multi-scale approach to the analysis of trends in a signal. The dominant trend is defined as the longest monotonically increasing or decreasing duration for each metric [33]. After detection of the dominant trend, explained in the next paragraph, we analysed its duration, start and terminal value and slope, and compared values for all groups. To detect the dominant trend in the values of all different parameters, the procedure as outlined in [33] was followed. It consists of 4 different steps, which are applied to

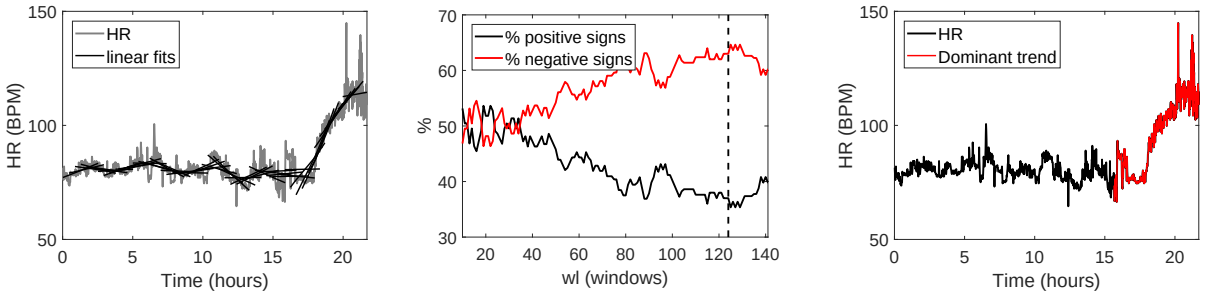

(a) Linear fit for one subwindow length *wl* in black, superimposed on the heart rate signal (grey).

(b) Percentage of positive vs negative signs for all values of *wl* together with the optimal *wl* (dotted line).

(c) Final result of dominant trend detection, with the dominant trend indicated in red.

Fig. 3: Illustration of the different steps in the detection of the dominant trend applied to a heart rate signal.

each series of parameter values. Since a tensor was constructed for each window of 100 heartbeats, the time scale of the parameter values is expressed in windows.

1) Let the sub-window length *wl* range from 10 to 150 windows. Create a set of overlapping sub-windows for each *wl* that span the entire recording with an increment of 1 window.
2) Perform robust linear fitting on each sub-window and record the signs of the slope of the linear fit. The sign that occurred most is the dominant slope sign. Robust linear fitting determines the best linear fit between the begin and endpoint of the sub-window while disregarding outliers in the signal.
3) Define the optimal sub-window length by calculating the sub-window length that contained the largest number of dominant slope signs.
4) The dominant trend is the interval that has the most number of consecutive dominant slope signs for the optimal window length.

When the dominant trend was detected, we easily determined its duration, slope, start and terminal value. The differences between values for different groups were tested with one-way Analysis of Variance (ANOVA) testing, followed by a post-hoc Tukey's honest significant difference test. ANOVA verifies whether means of parameter values in different categories are statistically different or not. If ANOVA yields statistically significant results, this indicates that at least one mean is significantly different. Tukey's honest significant difference test is a one-step multiple comparison test to compare all pairs of means that controls the family-wise error rate. For all tests a p-value <0.05 was considered significant.

Figure 3 illustrates the different steps in detection of the dominant trend. The signal depicted is a heart rate signal from the dataset with an obvious positive trend in the last quarter of the signal. On Figure 3a, the different robust fits for one sub-window length *wl* are plotted in black together with the heart rate signal. Figure 3b shows the percentage of positive and negative signs for each wl. Based on this figure the optimal window length is determined, indicated with a dotted line. The dominant trend is then detected in the signal, and shown on Figure 3c in red. Note that while the dominant trend is increasing, there can be periods within the trend where the heart rate instantly decreases (for instance around hour 16).

TABLE II: Results of the analysis of changes of feature values from baseline. The table represents the percentage (%) of patients in each group with significant increases or decreases in each parameter, together with the p-values from the corresponding Chi-Square test. Two parameters show significant differences between the three patient groups: PR-interval and QRS-interval prolongation. The parameters related to the changes in ECG wave amplitude change significant in a majority of patients over all groups.

Feature	All	VT/VF	Asystole	PEA	p-value
HR+	61,25	57,58	60,71	62,63	0,8737
HR-	25,00	24,24	25,00	25,25	0,9933
PR+	**45,00**	**63,64**	**50,00**	**37,37**	**0,0268***
PR-	38,13	39,39	50,00	34,34	0,3172
QRS+	**27,5**	**27,27**	**53,57**	**20,2**	**0,0023***
QRS-	15,63	15,15	25,00	13,13	0,3105
QTc+	65,00	66,67	67,86	63,64	0,8951
QTc-	58,13	57,58	67,86	55,56	0,5061
pAmp+	80,00	75,76	89,29	78,790	0,3732
pAmp-	74,38	72,73	85,71	71,72	0,3162
rAmp+	81,25	78,79	85,71	80,81	0,7748
rAmp-	66,88	57,58	60,71	71,72	0,2447
tAmp+	85,63	81,82	89,29	85,86	0,7055
tAmp-	72,50	69,70	67,86	74,75	0,7105

* denotes statistically significant results after correction for multiple comparisons with the Benjamini-Hochberg procedure.

V. Results

The results of both analyses are summarized in this Section. All calculations were performed in Matlab 2017b using Tensorlab for all tensor operations [34].

A. Changes from baseline

Table II shows the result for the first analysis, e.g. the changes compared to baseline values. All parameters changed significantly in at least 15% of all patients. QRS interval shortening was least often detected, T wave amplitude increase most often (85% of all patients). Remarkably, T wave

amplitude increase was also detected in 72.5%. Chi-square testing revealed significant differences between the 3 considered groups in two parameters: PR interval prolongation and QRS interval prolongation. Patients with VT/VF cardiac arrests had more increases in PR interval duration. Patients with asystolic arrests showed more increases in QRS interval length compared to other groups. PEA patients had a lower chance of PR and QRS prolongation compared to the other groups. For all groups, both increases and decreases in P, QRS and T wave amplitude were highly prevalent, with significant changes in more than $\frac{2}{3}$ of all patients overall. There were however no statistically significant differences between the different groups.

B. Dominant trend analysis

After detection of the dominant trend in all seven parameters, four characteristics of each dominant trend were compared between groups: the start value, terminal value, slope and duration. ANOVA testing showed significant differences for 6 parameters, presented in Figure 4. The terminal value and duration of the PR interval trend, the terminal value of the QRS interval trend and the begin- and terminal value and duration of the QTc interval trend. Tukey's hones significant difference test was used to examine which groups differed significantly from each other, results are indicated in Figure 4 with * (for $p<0.05$) and ** (for $p<0.01$). Results showed that all parameters were significantly different between either the VT/VF and PEA group (PR interval trend duration and all parameters derived from the QTc trends) or the asystole and PEA group (terminal values of PR and QRS interval trends).

VI. Discussion

This paper presents a method to automatically analyse changes in ECG morphology over time. The method was applied to a dataset of ECG signals of patients in the ICU to determine whether ECG morphology changes differently in patients with different causes of cardiac arrest.

First the changes compared to a baseline value in the beginning of the recording were analysed. The parameters that showed significant changes, PR and QRS interval prolongation, correspond with the findings of [8] where a similar analysis was done with manual measurements on a different dataset. Both baseline values and significant differences were defined identically to [8] so a valid comparison could be made. While QTc interval prolongation is no significant parameter in this dataset, the QTc interval increases in the majority of patients. This also matches the results in [8] and other similar studies [4]. When further analysing the changes in wave amplitude, it is remarkable that many signals showed both significant increases and decreases in the amplitudes of all ECG waves. This indicates that the ECG amplitude experiences many changes in the period before cardiac arrest that are larger than physiologically normal changes. While they were not discriminative between the groups considered in this experiment, they changed in a large majority of patients with cardiac arrests and might be therefore be of use for general patient monitoring.

When analysing the dominant trends in all parameters, six derived features showed significant differences between groups. The parameters where the dominant trend differed between the three groups largely correspond with the results of the first analysis: PR and QRS interval length. Differences in QTc interval trends were also significant, while this parameter was not picked up in the first analysis.

The start- and endpoint value as well as the duration of the trend in QTc interval length were all significantly larger in VT/VF patients than PEA patients. Since QTc prolongation is a known risk factor for Torsade de Pointes [35], a dangerous form of ventricular tachycardia, this result is not surprising. It is also supported by the findings in [4], [8].

When combining the results of both analyses, it can be concluded that changes in interval length are more significant between groups of patients with different causes of cardiac arrests than changes in amplitude. Changes in amplitude, especially for P wave and T wave amplitude, are however more prevalent overall and might thus be useful to monitor overall patient deterioration. To confirm this, it would be beneficial to collect data from a group of control patients that do not experience a code blue to verify the normal physiological variations in different parameters. This could be the subject of a follow-up study in order to transform the developed methods in useful clinical tools.

The Weighted Least-Squares approach used to compute the WCPD optimization problem is computationally much more efficient than previous weighted tensor decomposition methods. This is extremely beneficial for use in continuous patient monitoring, where the delay between the physiological change and the algorithmic output should be minimal. The current method gives an output for each sliding window of 100 heartbeats (1-1.5 minutes), resulting in a quasi-real time monitoring of ECG morphology. Recent advances in tensor methodology however focus on the development of efficient tensor *updating* methods [36], [37]. This class of methods calculate a new tensor decomposition every time new data arrives (for example after every heartbeat) in a time- and memory-efficient way. Their use would lead to an improvement in the time resolution of the results which could help in gaining a deeper understanding in the timing of the changes in ECG morphology before cardiac arrests.

VII. Conclusion

We have developed a tensor-based method to analyse changes in ECG morphology over time and used it to analyse changes prior to in-hospital cardiac arrests in three groups of patients, each with a different cardiac arrest mechanism. The results showed significant differences in multiple parameters with both analyses that largely confirm findings from previous studies. The developed methods work fully automated and are not dependent on the number of channels or measurement devices. Although a follow-up analysis using signals of control patients without cardiac arrests is necessary for validation, the current results show that the proposed tensor-based method leads to clinically valid results that are useful for identification of patients at risk for in-hospital cardiac arrest.

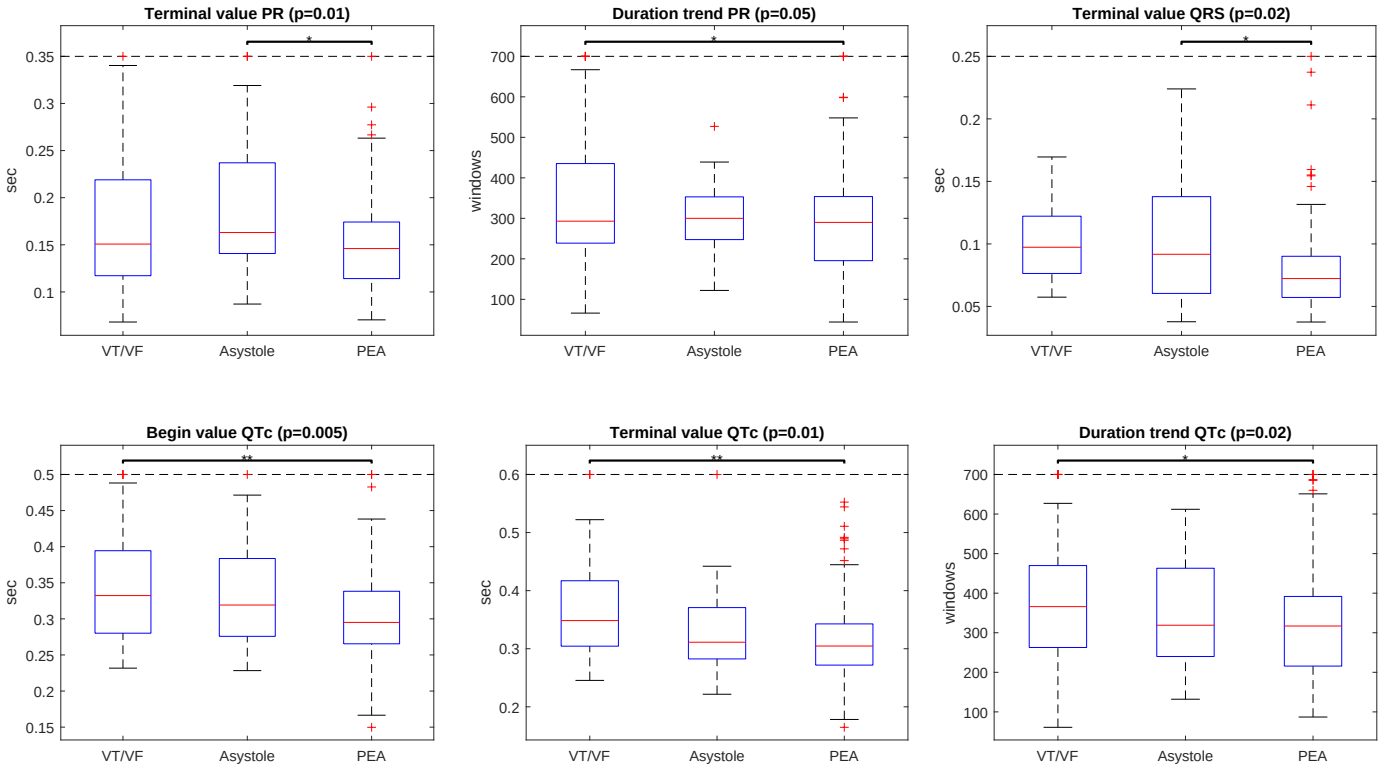

Fig. 4: Parameters derived from dominant trend analysis which showed statistically significant differences between all groups, together with the p-value results from one-way ANOVA. Results from Tukey's hsd test are indicated with * ($p<0.05$) and ** ($p<0.01$). Boxplots show median values and interquartile ranges. Outliers are clipped to improve visualization.

APPENDIX

In order to construct the weight tensor as explained in Section IV-C, a method to reliably estimate the quality of each heartbeat is necessary. For this we constructed a model that estimates the Signal-to-Noise ratio of each heartbeat based on different parameters. In literature, many methods can be found that estimate ECG signal quality, however a large number of these methods is not applicable in this case. For some quality estimators, such as [38], the goal is not to estimate the SNR, but mainly classify ECG signals as good or bad quality (e.g. clinically usable or not), which is not applicable in this case. Other methods require a longer period of ECG signal, using for example measures based on heart rate. Furthermore, methods that compare heartbeats to each other or to a template heartbeat are not desired either, since we expect heartbeat morphology to change over time due to changes in patient condition.

A. Construction of SNR model

To construct the model, we used the MIT-BIH Noise Stress Test Database [27] (available on Physionet [39]), which contains 12 half-hour ECG recordings from 2 subjects with SNR levels varying from -6dB to 24dB. The recordings were created by starting from 2 clean recordings and adding calibrated amounts of realistic ECG noise. Half of the available data (e.g. all heartbeats from all SNR levels from 1 subject) was used as a training set, the other half, consisting of all heartbeats from the second subject, as a test set. Based on the literature, 8 features were selected that have been shown to work effectively in estimating ECG signal quality, and that can be easily calculated based on 1 single-lead heartbeat:

1) Sample skewness s of a heartbeat $\mathbf{x}$:
$$s = \frac{E(\mathbf{x}-\mu)^3}{\sigma^3}$$
with μ and σ respectively the mean and standard deviation of the heartbeat $\mathbf{x}$.
2) Sample kurtosis k of a heartbeat $\mathbf{x}$:
$$k = \frac{E(\mathbf{x}-\mu)^4}{\sigma^4}$$
3) Power in 6 different subbands: 0-10 Hz, 10-20 Hz, 20-48 Hz, 48-52 Hz, 52-100 Hz, 100-120 Hz

All features were derived from the preprocessed ECG signal, e.g. after baseline wander removal and normalization (see Section IV).

A linear regression model was fitted using all heartbeats of the available training data, using the SNR labels provided in the dataset as predictor variable.

B. Validation of SNR model

The SNR model was first tested on the heartbeats in the test set of the MIT-BIH database. Afterwards it was further validated using a subset of the clinical dataset used in the remainder of the paper to verify whether the SNR model could be generalized for use on other datasets.

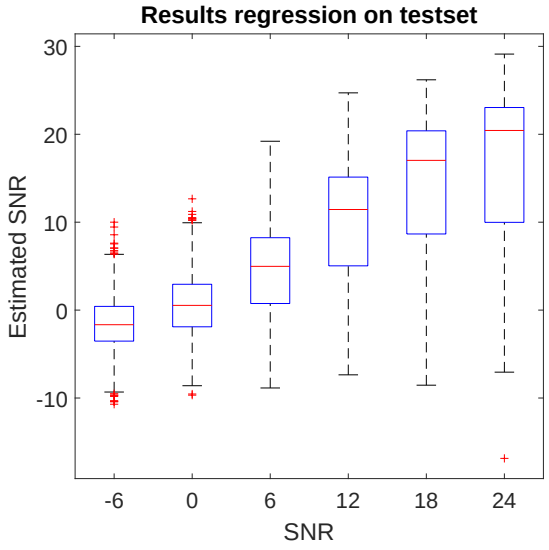

Fig. 5: Boxplots depicting the results of applying the SNR model on the test set. There is a clear correlation between the SNR values estimated by the proposed noise model and the true noise levels.

1) MIT-BIH Noise Stress Database: Figure 5 shows the result of applying the SNR model on the test set by SNR level. The Root Mean Square Error is 4.6dB. There is a clear correlation between the estimated SNR levels and the true SNR levels.

2) Clinical database: In order to verify whether the developed model can be applied on the current dataset (for which no reference SNR values are available), we selected 15 segments from 5 signals: 5 with good quality and no detectable artifacts, 5 with medium quality (some artifacts present, but ECG waves still clearly recognizable) and 5 with bad quality signal. Each segment contains approximately 100 heartbeats, resulting in 1500 heartbeats overall. Excerpts of all segments are shown in Figure 6. The SNR model was then used to calculate a quality estimate for each heartbeat in each segment. The results are presented as histograms for each class (clean, medium and noisy) and shown in Figure 7. It is clear that the different segments resulted in different SNR values. The heartbeats in the clean segment obtained a SNR value between 10 and 22, with an average of 15dB. The heartbeats in the segment with medium noise on the other hand had SNR values around 7dB and ranged between -2 and 18. Finally the very noisy segment had much lower SNR values, between -15 and 5.

To summarize, we developed a linear regression model to estimate the SNR value of individual heartbeats. The model uses 8 statistical and spectral features that lead to good results previously. The model was trained and tested on the MIT-BIH Noise Stress Database and validated on the clinical database. Results on both databases show that the model achieves good agreement with either reference SNR scores or visual analysis.

REFERENCES

[1] E. J. Benjamin et al. Heart Disease and Stroke Statistics-2017 Update: A Report From the American Heart Association. *Circulation*, 135(10):e146–e603, mar 2017.

[2] S. Girotra et al. Trends in Survival after In-Hospital Cardiac Arrest. *New England Journal of Medicine*, 367(20):1912–1920, nov 2012.

[3] F. C. Kempf and M. E. Josephson. Cardiac arrest recorded on ambulatory electrocardiograms. *The American Journal of Cardiology*, 53(11):1577–1582, jun 1984.

[4] A.B. de Luna, P. Coumel, and J.F. Leclercq. Ambulatory sudden cardiac death: Mechanisms of production of fatal arrhythmia on the basis of data from 157 cases. *American Heart Journal*, 117(1):151–159, jan 1989.

[5] E. Watanabe et al. Sudden cardiac arrest recorded during Holter monitoring: Prevalence, antecedent electrical events, and outcomes. *Heart Rhythm*, 11(8):1418–1425, aug 2014.

[6] Q. Ding et al. Developing new predictive alarms based on ecg metrics for bradyasystolic cardiac arrest. *Physiological measurement*, 36(12):2405, 2015.

[7] X. Hu et al. A casecontrol study of non-monitored ECG metrics preceding in-hospital bradyasystolic cardiac arrest: Implication for predictive monitor alarms. *Journal of Electrocardiology*, 46(6):608–615, nov 2013.

[8] D. H. Do et al. ECG changes on continuous telemetry preceding in-hospital cardiac arrests. *Journal of Electrocardiology*, 48(6):1062–1068, 2015.

[9] T. G. Kolda and B. W. Bader. Tensor Decompositions and Applications. *SIAM Review*, 51(3):455–500, 2008.

[10] A. Cichocki et al. Tensor Decompositions for Signal Processing Applications From Two-way to Multiway Component Analysis. *IEEE Signal Processing Magazine*, 32(2):145–163, 2015.

[11] N. D. Sidiropoulos et al. Tensor Decomposition for Signal Processing and Machine Learning. *IEEE Transactions on Signal Processing*, 65(13):3551–3582, jul 2017.

[12] G. Goovaerts et al. Automatic detection of T wave alternans using tensor decompositions in multilead ECG signals. *Physiological Measurement*, 38(8), 2017.

[13] S. Padhy and S. Dandapat. Validation of μ-volt T-wave alternans analysis using multiscale analysis-by-synthesis and higher-order SVD. *Biomedical Signal Processing and Control*, 40:171–179, feb 2018.

[14] S. Padhy and S. Dandapat. Third-order tensor based analysis of multilead ECG for classification of myocardial infarction. *Biomedical Signal Processing and Control*, 31:71–78, jan 2017.

[15] G. Goovaerts et al. Detection of irregular heartbeats using tensors. In *Computing in Cardiology*, volume 42, 2015.

[16] M. Boussé et al. Irregular heartbeat classification using Kronecker Product Equations. In *Proceedings of the Annual International Conference of the IEEE Engineering in Medicine and Biology Society (IEEE EMBS 2017), Jeju Island, South-Korea*, 2017.

[17] P. Paatero. A weighted non-negative least squares algorithm for three-way PARAFAC' factor analysis. *Chemometrics and Intelligent Laboratory Systems*, 38(2):223–242, oct 1997.

[18] M. Boussé and L. De Lathauwer. Nonlinear Least Squares Algorithm for Canonical Polyadic Decomposition Using Low-Rank Weights. In *IEEE 7th International Workshop on Computational Advances in Multi-Sensor Adaptive Processing (CAMSAP2017)*, pages 39–43, Curacao, Dutch Antilles, 2017.

[19] R. A. Harshman. Foundations of the parafac procedure: Models and conditions for an" explanatory" multimodal factor analysis. 1970.

[20] I. Domanov and L. De Lathauwer. Canonical polyadic decomposition of third-order tensors: Relaxed uniqueness conditions and algebraic algorithm. *Linear Algebra and its Applications*, 513:342–375, 2017.

[21] L. Sorber, M. Van Barel, and L. De Lathauwer. Optimization-based algorithms for tensor decompositions: Canonical polyadic decomposition, decomposition in rank-(l_r,l_r,1) terms, and a new generalization. *SIAM Journal on Optimization*, 23(2):695–720, 2013.

[22] I. Domanov and L. De Lathauwer. On the uniqueness of the canonical polyadic decomposition of third-order tensors—part ii: Uniqueness of the overall decomposition. *SIAM Journal on Matrix Analysis and Applications*, 34(3):876–903, 2013.

[23] G. Lenis et al. Comparison of baseline wander removal techniques considering the preservation of st changes in the ischemic ecg: a simulation study. *Computational and mathematical methods in medicine*, 2017, 2017.

[24] B. Iglewicz and D. Hoaglin. Volume 16: How to Detect and Handle Outliers. In *The ASQC Basic References in Quality Control: Statistical Techniques*, volume 16. 1993.

[25] C. A. Ledezma et al. A new on-line electrocardiographic records database and computer routines for data analysis. *Proceedings of Annual International Conference of the IEEE Engineering in Medicine and Biology Society.*, 2014:2738–2741, 2014.

[26] Debals O. and De Lathauwer L. The concept of tensorization. Technical report, KU Leuven, 2017.

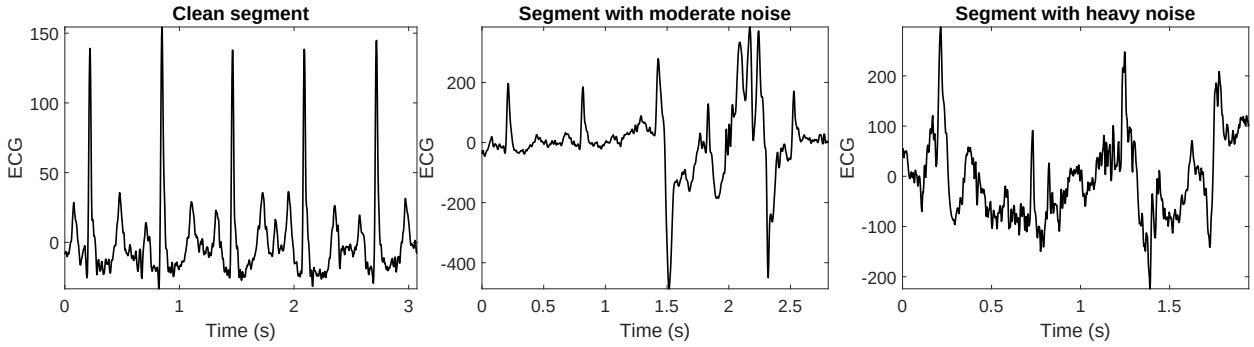

Fig. 6: Examples of segments of the same patient without noise (left), moderate noise (middle) and heavy noise (right). The clean segment contains no visual noise, the segment with moderate noise contains a considerate amount of baseline wander and the noisy segments is corrupted by both low- and high frequency artifacts.

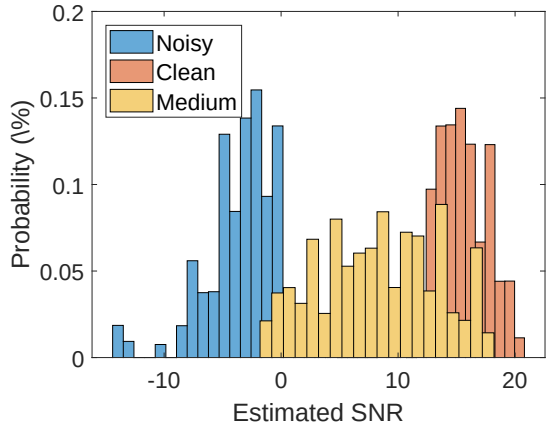

Fig. 7: Histograms of SNR values for each noise class: noisy (blue), medium (yellow) and clean (orange) heartbeats: The SNR values of noisy segments are clearly lower than clean segments, with intermediate values for medium quality segments.

[27] Moody, G.B., Muldrow W.E., and Mark R.G. The MIT-BIH Noise Stress Test Database. In *Computers in Cardiology*, pages 381–384, 1984.

[28] J. P. Martínez et al. A wavelet-based ECG delineator: evaluation on standard databases. *IEEE transactions on biomedical engineering*, 51(4):570–81, apr 2004.

[29] A. J. Moss. Measurement of the QT interval and the risk associated with QTc interval prolongation: A review. *The American Journal of Cardiology*, 72(6):B23–B25, aug 1993.

[30] C. Cammarota and M. Curione. Trend extraction in functional data of amplitudes of r and t waves in exercise electrocardiogram. *Fluctuation and Noise Letters*, 16(02):1750014, 2017.

[31] Y. Benjamini and Y. Hochberg. Controlling the false discovery rate: a practical and powerful approach to multiple testing. *Journal of the royal statistical society. Series B (Methodological)*, pages 289–300, 1995.

[32] J. H. McDonald. *Handbook of biological statistics*, volume 2. sparky house publishing Baltimore, MD, 2009.

[33] Q. Ding et al. Developing new predictive alarms based on ECG metrics for bradyasystolic cardiac arrest. *Physiological Measurement*, 36(12):2405–2422, dec 2015.

[34] N. Vervliet et al. Tensorlab 3.0, mar. 2016. *Available online. URL: https://www. tensorlab. net*.

[35] S. R. Beach et al. QTc Prolongation, Torsades de Pointes, and Psychotropic Medications. *Psychosomatics*, 54(1):1–13, jan 2013.

[36] M. Vandecappelle et al. Nonlinear least squares updating of the canonical polyadic decomposition. In *25th European Signal Processing Conference (EUSIPCO 2017), Kos, Greece*, pages 663–667, aug 2017.

[37] M. Vandecappelle et al. Cpd updating using low-rank weights. In *Proceedings of the 2018 IEEE International Conference on Acoustics, Speech and Signal Processing (ICASSP 2018), Calgary, Canada*, number accepted, 2018.

[38] J. Behar et al. ECG Signal Quality During Arrhythmia and Its Application to False Alarm Reduction. *IEEE Transactions on Biomedical Engineering*, 60(6):1660–1666, jun 2013.

[39] A. L. Goldberger et al. PhysioBank, PhysioToolkit, and PhysioNet: components of a new research resource for complex physiologic signals. *Circulation*, 101(23):E215–20, jun 2000.